Partitioning variance in population growth for models with environmental and demographic stochasticity

Jonas Knape*,[1] Matthieu Paquet[2] Debora Arlt[1]
Ineta Kačergytė[1] Tomas Pärt[1]

*jonas.knape@slu.se

[1]Swedish University of Agricultural Sciences

[2]University of Bordeaux

Abstract

1. How demographic factors lead to variation or change in growth rates can be investigated using life table response experiments (LTRE) based on structured population models. Traditionally, LTREs focused on decomposing the asymptotic growth rate, but more recently decompositions of annual 'realized' growth rates have gained in popularity.

2. Realized LTREs have been used particularly to understand how variation in vital rates translate into variation in growth for populations under long-term study. For these, complete population models may be constructed by combining data in an integrated population model (IPM). IPMs are also used to investigate how temporal variation in environmental drivers affect vital rates. Such investigations have usually come down to estimating covariate coefficients for the effects of environmental variables on vital rates, but formal ways of assessing how they lead to variation in growth rates have been lacking.

3. We extend realized LTREs in two ways. First, we further partition the contributions from vital rates into contributions from temporally varying factors that affect them. The decomposition allows us to compare the resultant effect on the

growth rate of different environmental factors that may each act via multiple vital rates. Second, we show how realized growth rates can be decomposed into separate components from environmental and demographic stochasticity. The latter is typically omitted in LTRE analyses.

4. We illustrate how to use the approach in an IPM for data from a 26 year study on northern wheatears (*Oenanthe oenanthe*), a migratory passerine bird breeding in an agricultural landscape. For this population, consisting of around 50-120 breeding pairs per year, we partition variation in realized growth rates into environmental contributions from temperature, rainfall, population density, and unexplained random variation via multiple vital rates, and from demographic stochasticity.

5. The case study suggest that variation in first year survival via the random component, and adult survival via temperature are two main factors behind environmental variation in growth rates. More than half of the variation in growth rates is suggested to come from demographic stochasticity, demonstrating the importance of this factor for populations of moderate size.

Keywords integrated population model; life table response experiment; growth rate; environmental stochasticity; demographic stochasticity

Introduction

Populations in the wild regularly experience changes in their environments, resulting in variation in demographic rates such as survival, birth and immigration rates. Life Table Response Experiments (LTREs) are a suite of methods developed with the aim of understanding how such change in demographic rates translate into variation in population growth (Caswell, 1989). The use of LTREs initially focused on decomposing changes in the asymptotic growth rate of stage or age structured deterministic matrix models into contributions from demographic rates, and also from environmental factors determining those rates. In a frequently changing environment asymptotic growth rates may, however, never be attained as constant perturbations hinder the population from approaching the stable stage structure associated with any particular environmental state. In such dynamic environments, LTREs based on asymptotic growth rates may not accurately capture the demographic causes of variation. For

instance, Koons et al. (2016) showed that the demographic factors highlighted as important in explaining variation in asymptotic growth rates by classical LTREs were not the same as those causing variation in the short term.

As an alternative to LTREs based on asymptotic growth rates, Koons et al. (2016) therefore considered LTREs decomposing variation in 'realized' growth rates into contributions from vital rates. The realized growth rate is simply the annual growth rate, and its variation is considered over a finite period of time such as the duration of a study period. One key difference between the classical LTREs and realized LTREs is that the latter includes effects due to variation in stage-structure, which does not affect asymptotic growth rates. Koons et al. (2016) called these 'transient LTREs'. Here we will instead refer to them as 'realized LTREs' to emphasize that they are not only useful in non-stationary environments or in a state away from equilibrium, but also to analyze population variation in stationary stochastic environments.

LTREs have often been used as a theoretical tool to gain a deeper understanding of already parametrized population models, but realized LTREs in particular also lend themselves well in an inferential context. Integrated population models (IPM, Besbeas et al., 2005; Plard et al., 2019) can be used to fit fairly complete structured population models by combining multiple types of demographic and population data. They therefore provide a framework for inferring a population model from a combination of demographic and census data in a coherent way. Using realized LTREs in combination with integrated population models, contributions of demographic vital rates to population growth can be estimated along with its uncertainty (Koons et al., 2017; Paquet et al., 2019).

IPMs can be used to investigate relations between temporal variation in environmental variables and variation in growth rates, mediated via demographic rates (Clark-Wolf et al., 2023; Weegman et al., 2017; Zhao et al., 2021). Such studies have usually used estimated covariate coefficients to assess the strength of environmental variables on demographic rates. A large coefficient does, however, not necessarily imply a large impact on the growth rate if the sensitivity of the vital rate is low. Similarly, opposing directions of effects of the same environmental variable on multiple vital rates can lead to unclear resultant effects on the growth rate (Canonne et al., 2023). Investigations into how environmental variation translates into variation in growth have been done with classical LTREs (Caswell, 2001) but rarely with realized LTREs. An exception is

Maldonado-Chaparro et al. (2018) who suggested regression on simulated population trajectories to decompose variation in annual growth into environmental contributions for integral projection models, but as far as we are aware such decompositions have not been used with integrated population models.

The aim of this paper is to explore a decomposition of variation in realized growth rates into contributions from environmental factors and density dependence acting via the vital rates, extending the methods of Koons et al. (2016). In addition we propose an approach to quantify the relative contributions of environmental and demographic stochasticity to variation in growth rates. We apply these decompositions to an IPM of northern wheatears (*Oenanthe oenanthe*), where we include temperature and rainfall during different periods of the annual cycle, as well as breeding period density dependence, as explanatory covariates for vital rate variation.

Methods

Scope

We consider a modelling framework where we have a structured population model with environmental variation and, possibly, demographic stochasticity. Environmental variation refers to temporal fluctuations in demographic rates across a population, and demographic stochasticity to chance events of demographic outcomes for individuals (Engen et al., 1998). Environmental variation can be captured by projection matrices A_t for each time step t which are determined by a set of vital rates. Below we will assume that t represents year, so that we have annual projection matrices. The vital rates determining the A_t matrices may vary over years and can be driven by environmental variables. In general we think of the annual vital rates as modelled with some link function for an appropriate scale (e.g. logit for survival probabilities), and with a linear predictor that may include population level annual environmental covariates and random effects. We also include the possibility of simple density dependence, e.g. via total population size, in the linear predictors. This framework covers common types of models inferred via fitting integrated population models (Schaub & Kéry, 2021).

Contributions from population structure and environmental variation

We start by considering only environmental variation in population dynamics, and decompose variation in realized growth rates into contributions from population structure (in terms of age or stage), density dependence and environmental factors. In a later section we will also consider demographic stochasticity.

Under environmental variation only, age or stage structured population dynamics are fully described in terms of the annual projection/transition matrices A_t, and $n_{t+1} = A_t n_t$, where n_t is a vector containing the population numbers in the different ages or stages. The realized annual growth rate (as defined in Koons et al. (2016)) is then

$$\lambda^{ES}_{\text{real},t} = \frac{||A_t n_t||}{||n_t||} = ||A_t \tilde{n}_t||$$

where $||\cdot||$ is the *l1* vector norm (i.e. the total of all elements in the vector) and $\tilde{n}_t$ is the normalised population age or stage-structure vector. We use the superscript ES to highlight that this growth rate is determined by the state of the environment (A_t) and by the stage structure.

Koons et al. (2016) used a Taylor approximation of $\lambda^{ES}_{\text{real},t}$ to break down its variance $V(\lambda^{ES}_{\text{real},t})$ into contributions from time varying vital rates. The same type of first order Taylor approximation is also commonly used for computing classical LTREs of deterministic asymptotic growth rates (Caswell, 2001). For these classical LTREs the first order approximation has further been used to compute contributions from environmental factors acting on the vital rates. We use the same approach here, but apply it to realized annual growth rates instead of deterministic asymptotic growth rates.

To help illustrate the approximation we write the annual realized growth rate as a function of all its underlying time varying parameters:

$$\lambda^{ES}_{\text{real},t} = f(\theta_t)$$

so that $\lambda^{ES}_{\text{real},t}$ is completely determined by θ_t. A first order Taylor expansion around the mean of θ gives

$$f(\theta) \approx f(\bar{\theta}) + \nabla f^T_{\bar{\theta}} \ (\theta - \bar{\theta})$$

where $\nabla f_{\bar{\theta}} = (\frac{\partial f}{\partial \theta_1}|_{\bar{\theta}}, \cdots, \frac{\partial f}{\partial \theta_k}|_{\bar{\theta}})$ is the gradient of f evaluated at the (temporal) mean of the vector θ, and T denotes vector transpose. Using rules for how to compute the variance of a vector of random parameters multiplied by a fixed vector, the variance of f can be approximated as

$$\mathrm{Var}(f(\theta)) \approx (\nabla f)^T_{\bar{\theta}} \Sigma_\theta (\nabla f)_{\bar{\theta}}$$

where Σ_θ is the covariance matrix of θ. This is identical to a delta approximation (Ver Hoef, 2012) for the variance of the function f given the covariance matrix of its parameters.

The formula can be used to define contributions to the variance from each θ_i by summing the variance and covariance terms involving θ_i

$$\mathrm{contribution}(\theta_i) = V(\theta_i) \left(\frac{\partial f}{\partial \theta_i} \right)^2 + \sum_{j \neq i} \mathrm{Cov}(\theta_i, \theta_j) \frac{\partial f}{\partial \theta_i} \frac{\partial f}{\partial \theta_j}$$

These contribution sum to the total (approximate) variance of $\lambda^{ES}_{\mathrm{real}}$, and relative contributions can be computed through dividing by this total variance. Covariances between pairs of distinct parameters are given equal weights in their respective contributions, and contributions for some parameters can become negative when the covariance terms are negative and dominate the variance, which can make interpretation difficult. A computationally convenient formula to simultaneously calculate all contributions is

$$\mathrm{contribution}(\theta) := \nabla f_{\bar{\theta}} \circ \Sigma_\theta \ \nabla f_{\bar{\theta}}$$

where $\circ$ denotes element-wise multiplication (Hadamard product).

Koons et al. (2016) treated the θ_t as the set of all time varying vital rates (e.g. reproduction and survival at different ages) plus the elements of the population structure vectors. To decompose the variance further we can instead think of θ as containing time varying components of the linear predictors that determine the time varying vital rates, plus the population structure. As an example, suppose we model first year survival as a function of population density, a covariate x and a random effect,

$$\mathrm{logit}(\phi_{0,t}) = \mu + \beta x_t + \gamma ||n_t|| + \epsilon_t,$$

then the time varying components of this linear predictor are βx_t, $\gamma||n_t||$, and ϵ_t. If we collect all such terms across all time varying vital rates and add the population structure, $\lambda_{\text{real},t}$ is again completely determined by θ and we can use the variance approximation formula to decompose the variance of the realized growth rate into contributions from the terms in the linear predictors. To do this, we need to compute the gradient $\nabla f_{\bar{\theta}}$ and the covariance matrix Σ_θ. The gradient $\nabla f_{\bar{\theta}}$ is usually straightforward (but potentially tedious) to compute as $\lambda^{ES}_{\text{real},t} = ||A_t\tilde{n}_t||$ tend to contain simple terms (sums of products between vital rates and population structure) that are easy to differentiate (Appendix C). This gradient is similar to the gradient when the θ are treated as vital rates (Koons et al., 2016) but with the addition that we also need to take the derivative of the inverses of any link function. The covariance matrix Σ_θ can be estimated by the sample covariance matrix of the full θ vector across time. With IPMs, which are typically implemented using MCMC in a Bayesian framework, it is easy to set up computations so that all the elements of θ are directly available and the covariance matrix can then be computed for each posterior iteration to give a posterior distribution of the contributions.

Diagnosing the linear approximation The approximation used to break down variation in $\lambda^{ES}_{\text{real}}$ into its contributing components will not work well if there is strong non-linearity in the relationships between the components and the growth rate over the range of the variation in the components. Fortunately, the performance of the approximation can be easily checked by comparing the variance of $\lambda^{ES}_{\text{real, t}}$ to its total variation as indicated by the approximation (sum of all its contributions)(Caswell, 2001; Koons et al., 2017). This comparison is also useful for diagnosing coding errors or incorrect calculations of derivatives.

Measuring contributions of demographic stochasticity

Demographic stochasticity can be included in population models using distributions that describe outcomes of life-history events at the individual level. For instance, annual survival of an individual may be modelled as a Bernoulli trial and, assuming independence and identical rates among individuals in the same stage in the population, the total number of survivors in a life-stage has a binomial distribution.

In this situation, we define the matrix A_t as the expected projection matrix in year t

given the environment (and population size) where the expectation is taken over the demographic stochasticity. In other words, we define A_t using the expected vital rates in year t, e.g. the expected survival probability of an age class. The population vector n_{t+1} is then no longer equal to $A_t n_t$ and we define

$$\lambda_{\text{real},t} = \frac{||n_{t+1}||}{||n_t||} = \frac{||A_t n_t|| + D_t}{||n_t||} = \lambda^{ES}_{\text{real},t} + \lambda^{D}_{\text{real},t}$$

where $D_t = ||n_{t+1}|| - ||A_t n_t||$ is the difference between actual population size and the projected population size we would expect from environmental variation alone. D_t denotes the total effect of demographic stochasticity and can be a complex quantity involving products or sequences of demographic stochasticity from multiple vital rates. Note that λ^D unlike λ^{ES} can be both negative and positive (this would be avoided if the decomposition is defined at the log-scale). For large n, λ^D should become small.

We then use

$$\frac{V(\lambda^{ES}_{\text{real},t}) + \text{Cov}(\lambda^{ES}_{\text{real},t}, \lambda^{D}_{\text{real},t})}{V(\lambda_{\text{real},t})}$$

as a measure of the relative contribution of environmental variation and population structure to variation in the realized growth rate, and, correspondingly,

$$\frac{V(\lambda^{D}_{\text{real},t}) + \text{Cov}(\lambda^{D}_{\text{real},t}, \lambda^{ES}_{\text{real},t})}{V(\lambda_{\text{real},t})}$$

for the relative contribution of demographic stochasticity. Covariance terms are included so that the sum of the two relative contributions is 1.

Case study using transient LTREs with integrated population models

The above decompositions can be used in combination with inference via integrated population models. We will illustrate this in a case study where we first compute the contribution of environmental covariates, density dependence and population structure to variation in λ^{ES} as in the previous section, and then separately estimate the relative magnitude of environmental and demographic variation. For the case study we use field data from 26 years (1993 to 2018) from a population of wheatears, a migratory bird species wintering in the Sahel region and breeding in an agricultural landscape near Uppsala in Sweden. We use mark-resighting data of birds ringed either as adults or as chicks in the nest, data on reproductive performance, and census data on occupied

breeding territories to parametrize an age structured population model by combining data in an integrated population model. The model describes the number of young (one year old) and old (2 years and older) males each year in a pre-breeding census formulation. We choose these two age classes because they display the most prominent differences in vital rates (e.g. Pärt, 2001), and we only consider males as they are easy to categorize as young or old whereas the same female age classes are harder to determine. Details of the wheatear study system and of how data are handled and combined in the IPM are provided in Appendix A, and we focus below on the annual dynamics resulting from the IPM.

Annual transition matrix The basic structure of the annual projection matrix A_t, without demographic stochasticity, is

$$A_t = \begin{pmatrix} \nu_{1,t} r \psi_t \phi_{0,t} + \omega_{1,t} & \nu_{2,t} r \psi_t \phi_{0,t} + \omega_{1,t} \\ \phi_{1,t} + \omega_{2,t} & \phi_{2,t} + \omega_{2,t} \end{pmatrix}$$

Briefly, $\nu_{1,t}$ and $\nu_{2,t}$ represent the probability of early nest survival from initiation of breeding until chicks are approximately 6 days old for young (1) and old (2) male parents, r is the expected number of 6 day old chicks produced per nest, ψ_t is the survival probability of nestlings until fledging (from 6 days old until 15 days when they fledge), $\phi_{0,t}$ is first year apparent survival probability after fledging and includes the probability that the bird is a male (because chicks cannot be sexed in the field, see Appendix A), $\phi_{1,t}$ and $\phi_{2,t}$ are apparent survival probabilities of young and old males, and $\omega_{1,t}$ and $\omega_{2,t}$ are immigration rates into the young and old age classes (see Table 1 for a more precise definition of the vital rates). Except for r which is estimated as a fixed parameter among years, these vital rates are modelled via link functions (logistic for survival probabilities and exponential for immigration rates) as depending on environmental covariates, density dependence and annual random effects. For early nest survival and nestling survival we used local rain and temperature during those stages as covariates, for first year survival after fledging we used breeding population density and rainfall in the wintering area, and for young and old male survival we used local rainfall and temperature in summer as well as rainfall in the wintering area (Table 1). Further motivation behind the choice of environmental covariates is given in Appendix A.

Demographic stochasticity To incorporate demographic stochasticity, we consider each vital rate in the matrix A_t to be the expectation of a random variable capturing variation in the outcomes of individual life-history events. These random variables representing demographic stochasticity are modelled with binomial distributions for early nest survival and nestling survival, and for first year, young male and old male survival, and with Poisson distributions for the number of chicks and the number of immigrants into each age class. As a consequence, the total number of young males in year $t+1$, $n_{1,t+1}$, is the sum of the result of a sequence of binomial and Poisson draws involving young males breeding in year t, a sequence of draws involving old males breeding in year t and immigration via a Poisson$((n_{1,t}+n_{2,t})\omega_{1,t})$ distributed variable. Likewise, the number of old males in year $t+1$, $n_{2,t+1}$, is the sum of a Binomial$(n_{1,t},\phi_{1,t})$, a Binomial$(n_{2,t},\phi_{2,t})$, and a Poisson$((n_{1,t}+n_{2,t})\omega_{2,t})$ distributed variable.

Model fitting details We formulate the model in a Bayesian framework and therefore need priors for model parameters. For regression coefficients at the logit scale we used normal priors with zero mean and standard deviation 1.5 for intercepts and 1 for covariate slopes. We used uniform priors over $(0,1)$ for detection probabilities, and a uniform prior over $(0,8)$ for r.

For vital rates for which there are no direct observed data, typically immigration as in our case, contributions tend to get inflated when temporal random effects for them are modelled (Paquet et al., 2021). To reduce this effect we put exponential shrinkage priors (rate = 20) on the random effect standard deviations (for all vital rate random effects, not only immigration). These priors aim to reduce model complexity (Simpson et al., 2017) by shrinking variation towards zero. As a consequence, a small posterior random effect variance does not necessarily mean that the variation in the parameter is small, but simply that there is no evidence of strong variation.

We also put a shrinkage prior on the intercepts for immigration (rate = 10) as we don't have direct data on immigration which might lead to unstable estimation of this parameter.

The IPM was implemented in NIMBLE (Valpine et al., 2016) using 4 MCMC chains, each with 21000 iterations and discarding the first 1000 iterations (code in Supplement 1). For each iteration of the MCMC output we computed contributions from each

component of the linear predictors of the vital rate, and from age structure, to yield the posterior distribution of the contributions. Convergence of the MCMC was assessed using the R-hat statistic on the 4 chains. These were all below 1.03.

Model fit was assessed by posterior predictive p-values (Appendix B). The fit was acceptable for most aspects of the model that we investigated. However, the number of chicks was underdispersed relative to the Poisson distribution we used. Attempts to reconcile this with a multinomial distribution resulted in numerical problems for the MCMC sampler, and we therefore kept the Poisson distribution.

In addition to the main model we considered an alternative with a different specification of nestling survival. The alternative model assumed that variation in nestling survival was due to deaths of individual young in the nest, as opposed to total nest failure in the main model (see Appendix A and B for further discussion).

The age-structure vector in our case has two components that sum to 1, so that there is only one degree of freedom in its variation. We therefore parameterized $\lambda^{ES}_{\text{real},t}$ as a function of $\tilde{n}_{1,t}$ only (i.e. with $\tilde{n}_{2,t}$ replaced by $1-\tilde{n}_{1,t}$) when computing the gradient and contributions.

Results of case study

The population declined over the study period with a marked variation in annual growth rates (Fig. 1). Decomposing the variance in the realized growth rate without demographic stochasticity (λ^{ES}) into contributions from vital rates (similarly to Koons et al., 2016, 2017) suggests that most of the variation comes from first year survival, and with smaller contributions from survival of old and young males and nestlings (Fig. 2). Early nest survival and immigration both have small contributions, and variation in age structure contributed almost nothing to variation in growth.

Breaking the contributions down into environmental components affecting the vital rates suggests that random effects and winter rain for first year survival and summer temperature for survival of old males provide the largest contributions to environmental variation in the growth rate (Fig. 3). The effects of these two rain and temperature covariates are however uncertain (Fig 4). There is a clearer effect for summer temperature on nestling survival, but the resulting contribution to variation in growth is small.

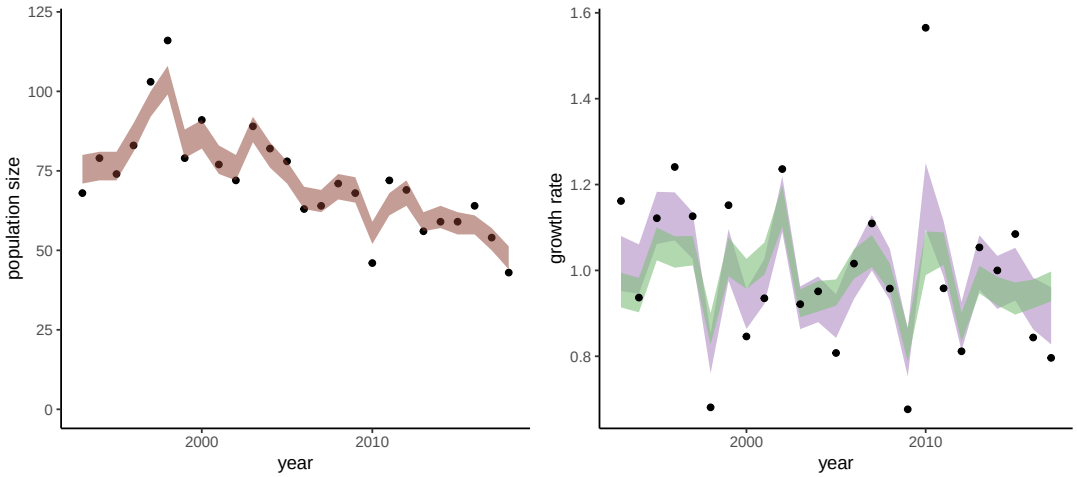

Figure 1: Left panel: Observed (points) and estimated (shaded area, showing 50% credible intervals) population size over the study period. Right panel: Observed (points) and estimated (shaded areas, showing 50% credible intervals) annual growth rates. The green shaded area shows estimated annual growth rates including environmental variation and variation in age structure (i.e. λ^{ES}), the purple shaded area shows estimated growth rate also including demographic stochasticity (i.e. $\lambda^{\mathrm{ES}} + \lambda^{\mathrm{D}}$).

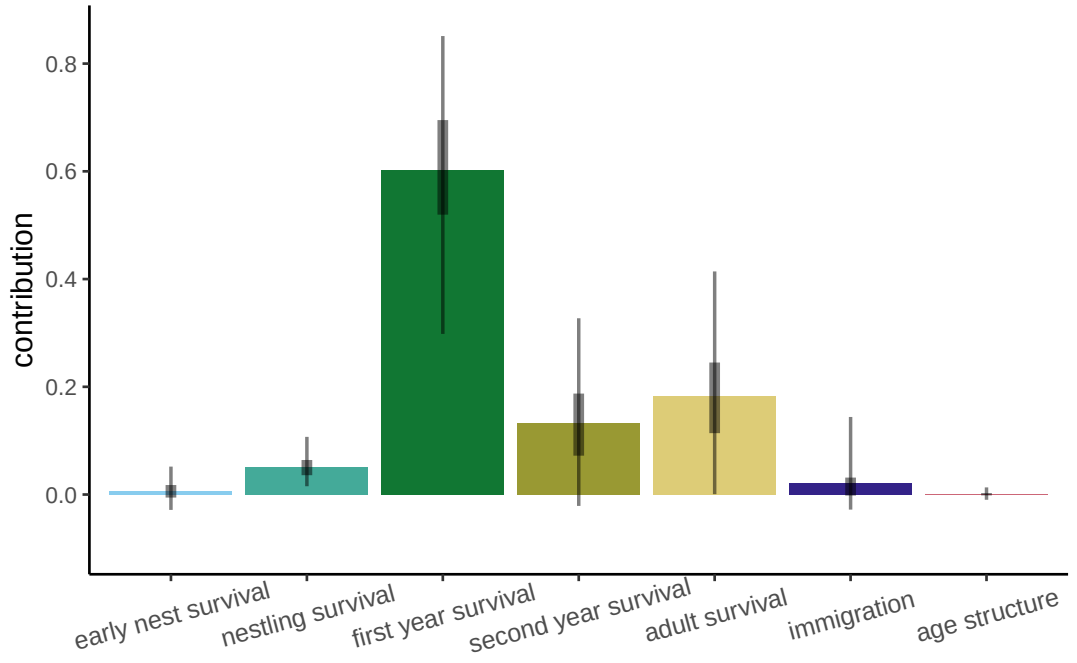

Figure 2: Total relative contributions to environmental variance in the realized growth rate for each vital rate (summed across all linear predictor components of the vital rates). Error bars show 50% (thick) and 95% (thin) credible intervals.

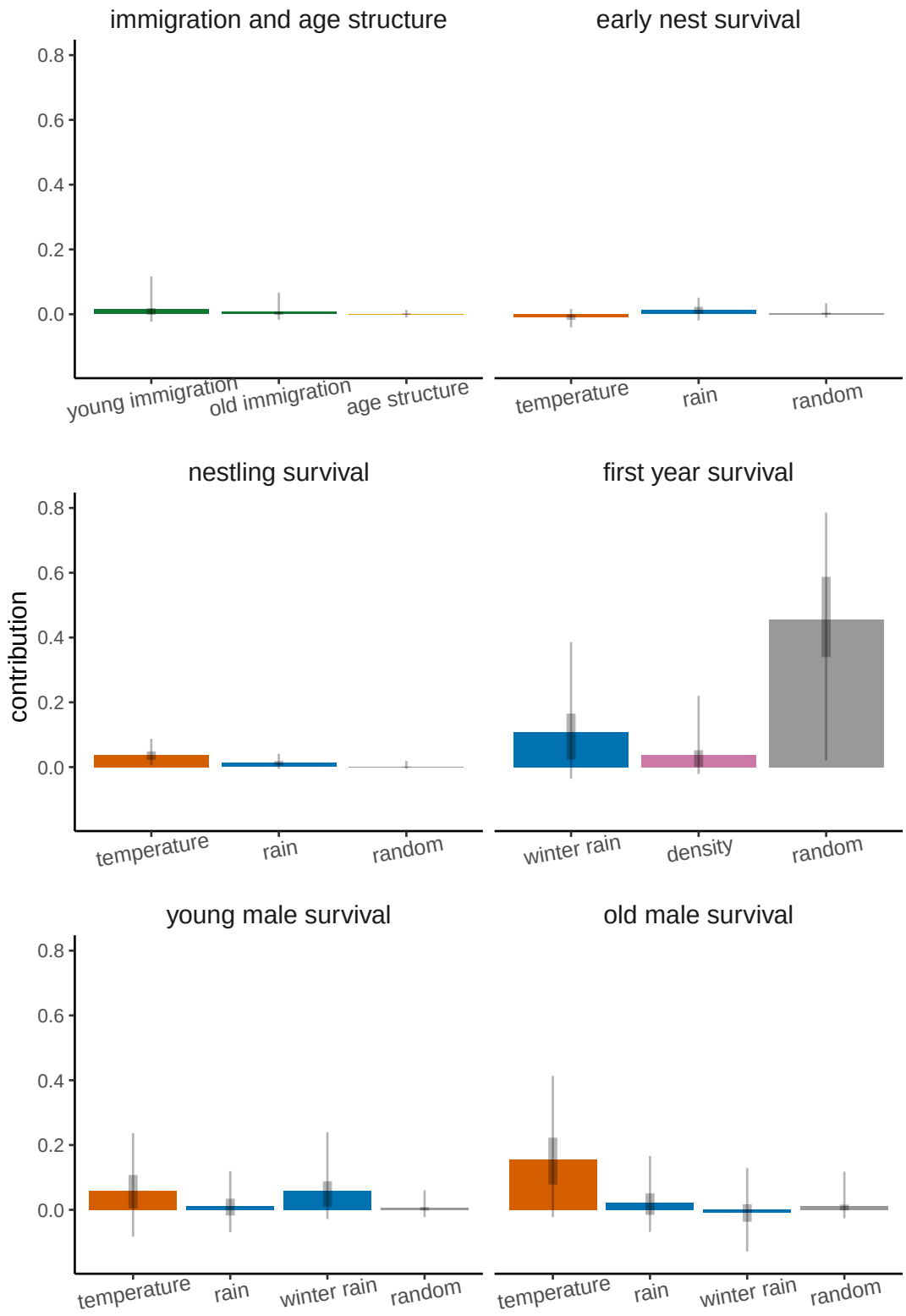

Figure 3: Relative contributions (summing to 1) to environmental variation in the realized growth rate from all linear predictor components and vital rates. Error bars show 50% (thick) and 95% (thin) credible intervals.

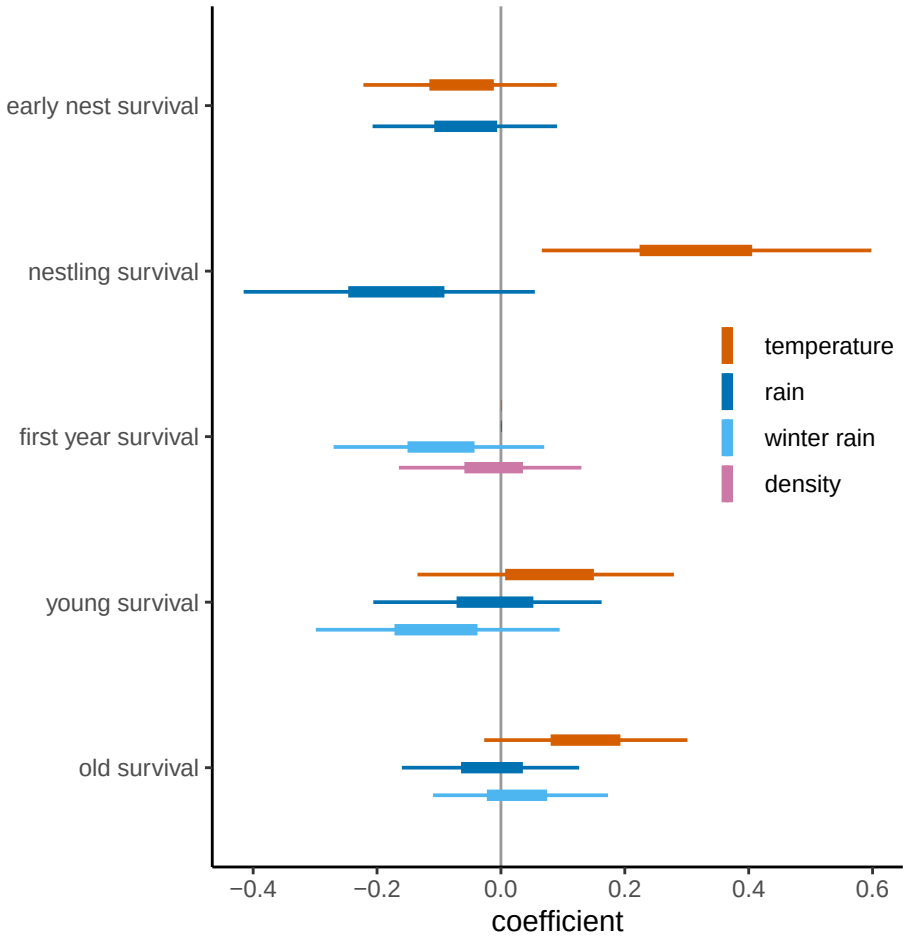

Figure 4: Estimated slopes for all environmental covariates on vital rates. Error bars show 50% (thick) and 95% (thin) credible intervals.

Alternatively, we may compute total contributions of different groups of variables that may act across different vital rates. For example, Fig. 5 shows total contributions of weather, density, random effects, and population structure to the variance in the realized growth rate, showing that roughly equal portions of the variance are due to weather and random effects in the model. The weather contributions were computed by summing contributions from all temperature and rainfall covariates across all vital rates, and the random effect contributions by summing all random effects components across all vital rates (including immigration).

Comparing the actual variance of λ^{ES} to the approximated variance (i.e. the sum of all contributions) shows that the approximation slightly underestimated the actual variance with a relative error of -2% on average over the posterior distribution, but with larger errors for some posterior draws (95% CI: -16% - 14%).

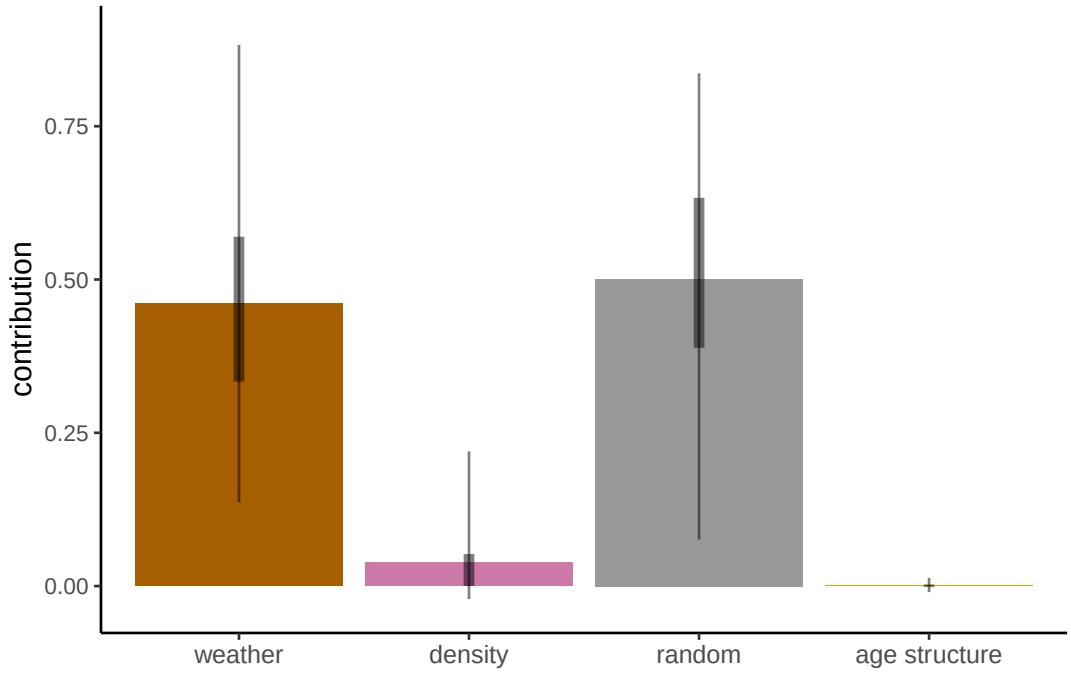

Figure 5: Relative contributions from weather (rainfall and temperature), population density, random effects (including for immigration), and age structure to environmental variance in realized growth. Error bars show 50% (thick) and 95% (thin) credible intervals.

The above results show contributions to environmental variation in growth only. If we consider the population across the censused area, which has around 50-120 individual males per year, demographic stochasticity accounts for a large portion of the variance

in the realized growth rate. Specifically the contribution of demographic stochasticity via λ^D is ca 56% (95% CI: 31-84%), while the remaining contribution is due to variation in λ^{ES}, i.e. environmental variation and, to a very small extent, variation in age structure.

In the alternative model where variation in nestling survival is assumed to be due to death of individual chicks instead of total nest failure (Appendix B), there is a large contribution of nestling survival to variation in growth, and a smaller contribution from first year survival compared to the main model (Fig 6). In this model, the contributions from temperature and rainfall via nestling survival are also larger (Fig 7). Because distinguishing the two models is difficult (Appendix B), it is not fully clear during which part of the time period from the ringing of chicks to their return the following year that some of the variation contributing to variation in growth occurs.

Discussion

Studies using LTREs to decompose variance in realized growth rates with IPMs have focused on contributions from variation in vital rates, even when environmental predictors have been included in models (e.g. Canonne et al., 2023; Nater et al., 2022). We show how realized LTREs can be used to also decompose variation into contributions from environmental factors, and to assess the overall contribution of environmental versus demographic stochasticity, two conceptual extensions of the approach of Koons et al. (2016).

Estimating contributions

The decomposition of environmental variation relies on approximating the (environmental) realized growth rate using a first order Taylor expansion, which may not be accurate if there is strong environmental variation or strong non-linearity in the response to the environment. In our case study the average relative error was a modest -2%, but was higher over parts of the posterior distribution. Alternative decompositions to try to reduce error have been suggested. Rees & Ellner (2009) suggested LTREs of the realized growth rate for integral projection models that rely on multiple regression growth rates against vital rates for simulated population dynamics. This approach has been extended to LTREs of environmental factors determining the vital

rates, also for integral projection models (Maldonado-Chaparro et al., 2018). It differs from the approach taken here in that a simulation scheme for hypothetical environmental variables as well as regression model to analyze the simulated growth rates need to be set up. In contrast, Taylor approximation based LTREs are directly derived from the model and no design choices are necessary in the calculation of contributions. Another difference is that while we estimate only direct effects on the growth rate, Maldonado-Chaparro et al. (2018) try to also estimate lagged effects of environmental variables. Such lagged effects would appear in the age structure contributions of our approach.

Another alternative is to use functional decompositions (Hooker, 2007) as a basis for LTREs. Hernández et al. (2023) proposed this approach and used it to decompose differences in the asymptotic growth rate between different treatments. It could, in theory, be used to approximate the variance in realized growth rates to an arbitrary degree of precision by increasing the order of the functional expansion, but in practice computation time and interpretation will be limiting factors (Hernández et al., 2023). As far as we are aware none of these two alternative decompositions have yet been used with IPMs, but it appears straightforward to apply them also in that setting. It is unclear to us if they would perform better than the Taylor approximation based LTREs. We suggest that the more direct Taylor based or functional decomposition approaches could be used in first attempts to compute contributions from environmental variables. In cases where the performance turns out to be poor, a simulation approach (Maldonado-Chaparro et al., 2018) could be considered.

To measure contributions from demographic stochasticity we compare the growth rate when random outcomes from all the model components that represent demographic stochasticity are included to the expected growth rates when these components are fixed at their annual means. The relative effect of the demographic stochasticity components will decrease with population size and hence the relative contribution of demographic stochasticity will depend on the size of the population that is considered. In an IPM with census data, an obvious choice is to estimate the contribution of demographic stochasticity for the population that is being censused. However, the contribution of demographic stochasticity could be predicted more generally by simulating the outcomes of demographic events for a population of any given (initial) size.

Case Study

For the wheatear population model, an LTRE decomposition into vital rate contributions suggests that environmental variation in annual growth rates mainly comes from variation in first year survival after fledging and in survival of old males (Fig. 1). Further decomposing these contributions into components from environmental variables shows that the contribution from first year survival is mainly linked to unexplained random variation while the contribution from old male survival is related to summer temperatures. In total, slightly less than half of the environmental variation in growth were explained by weather covariates while the other half came from the unexplained random components. Another new aspect of our IPM analysis is that we also quantify the magnitude of demographic stochasticity, and a large portion of the variance in the realized growth rate seems to come from this component.

The importance of first year and adult survival is partly in agreement with a previous realized LTRE analysis of vital rates in this population using a different model (Paquet et al., 2019). Our results are also partly compatible with previous analyses of weather variables in the wheatear population, conducted at an individual level rather than at the population level adopted here. These suggested, among other things, that rainfall during the nestling period reduced fledging success and that temperature increased it (Öberg et al., 2015). Our results point in the same direction although the negative effect of rainfall was uncertain in the main model. The implications on variation in population growth however was strongly dependent on the specification of the nestling survival model. In the main model the contribution from these weather effects via nestling survival were very small, but substantial in the alternative model. This shows how seemingly innocuous model specification choices, in this case whether variation in nestling survival was due to complete nest failure or to death of individual chick, can sometimes lead to substantial differences in contributions.

In contrast to several other studies (Millon et al., 2019; Nater et al., 2022; e.g. Weegman et al., 2017), including the previous IPM study on wheatears (Paquet et al., 2019), our results suggest limited contribution of immigration to annual variation in growth rates. We believe this is mainly a consequence of our use of penalized complexity priors for random effects variances. Using an uninformative weak prior for immigration will often result in a large contribution because direct information about immigration is typically missing and the error term adjusts to any discrepancy between the growth

rate projected from the vital rates and the growth rate inferred from survey data (Paquet et al., 2021). Penalized complexity priors are a convenient way of mitigating this effect.

The large contribution from demographic stochasticity (56%) may seem high, but is not unreasonable for a population of this size (~100 males, c.f. Lande et al., 2003; Steiner et al., 2021), although in our case the estimate of demographic stochasticity may be inflated to some extent since we had to resort to a Poisson distribution for computational reasons. Nevertheless, estimating environmental variability in demographic rates from study populations of limited size is a challenge because its signals can be obscured by demographic stochasticity, even for long term studies (Ross & Weegman, 2022). This may partly explain the large uncertainty often seen in estimated contributions, here and in other studies.

Conclusions

LTRE analyses of realized growth rates have been used to shed light on how variation in vital rates over a study period contribute to population change. The methods illustrated here provide a means of assessing how these contributions are mediated by lower level environmental drivers, and additionally determining contributions from demographic stochasticity. They can give us a more complete picture of the different paths along which a population model moderates fundamental sources of variation into variation in population growth.

Author contributions JK and MP conceived the initial idea for the study. JK analysed data, with input from all authors, and wrote the original draft. TP initiated the field study, DA and TP led the study and curated data. DA extracted initial data for analysis. All authors contributed to revisions of the text.

References

Arlt, D., Forslund, P., Jeppsson, T., & Pärt, T. (2008). Habitat-Specific Population Growth of a Farmland Bird. *PLoS ONE*, *3*(8), e3006. https://doi.org/10.1371/journal.pone.0003006

Arlt, D., Olsson, P., Fox, J. W., Low, M., & Pärt, T. (2015). Prolonged stopover duration characterises migration strategy and constraints of a long-distance migrant

songbird. *Animal Migration*, *2*(1), 47–62. https://doi.org/10.1515/ami-2015-0002

Arlt, D., & Pärt, T. (2017). Marked reduction in demographic rates and reduced fitness advantage for early breeding is not linked to reduced thermal matching of breeding time. *Ecology and Evolution*, *7*, 10782--10796. https://doi.org/10.1002/ece3.3603

Besbeas, P., Freeman, S. N., & Morgan, B. J. T. (2005). The potential of integrated population modelling. *Australian & New Zealand Journal of Statistics*, *47*(1), 35–48. https://doi.org/10.1111/j.1467-842X.2005.00370.x

Canonne, C., Bernard-Laurent, A., Souchay, G., Perrot, C., & Besnard, A. (2023). Contrasted impacts of weather conditions in species sensitive to both survival and fecundity: A montane bird case study. *Ecology*, *104*(2), e3932. https://doi.org/10.1002/ecy.3932

Caswell, H. (1989). Analysis of life table response experiments I. Decomposition of effects on population growth rate. *Ecological Modelling*, *46*(3), 221–237. https://doi.org/10.1016/0304-3800(89)90019-7

Caswell, H. (2001). *Matrix population models* (2nd ed.). Sinauer Associates.

Clark-Wolf, T. J., Dee Boersma, P., Rebstock, G. A., & Abrahms, B. (2023). Climate presses and pulses mediate the decline of a migratory predator. *Proceedings of the National Academy of Sciences*, *120*(3), e2209821120. https://doi.org/10.1073/pnas.2209821120

Cramp, S. (1988). *Handbook of the Birds of Europe, the Middle East and North Africa. The Birds of the Western Palearctic. Vol. 5: Tyrant Flycatchers to Thrushes*. Oxford University Press.

Engen, S., Bakke, Ø., & Islam, A. (1998). Demographic and Environmental Stochasticity-Concepts and Definitions. *Biometrics*, *54*(3), 840–846. http://www.jstor.org/stable/2533838

Hernández, C. M., Ellner, S. P., Adler, P. B., Hooker, G., & Snyder, R. E. (2023). An exact version of Life Table Response Experiment analysis, and the R package exactLTRE. *Methods in Ecology and Evolution*, *n/a*(n/a). https://doi.org/10.1111/2041-210X.14065

Hooker, G. (2007). Generalized Functional ANOVA Diagnostics for High-Dimensional Functions of Dependent Variables. *Journal of Computational and Graphical Statistics*, *16*(3), 709–732. https://doi.org/10.1198/106186007X237892

JISAO. (2018). *Sahel Precipitation Index* [Data set]. https://doi.org/10.6069/H5MW2F2Q

Koons, D. N., Arnold, T. W., & Schaub, M. (2017). Understanding the demographic drivers of realized population growth rates. *Ecological Applications*, *27*(7), 2102–2115. https://doi.org/10.1002/eap.1594

Koons, D. N., Iles, D. T., Schaub, M., & Caswell, H. (2016). A life-history perspective on the demographic drivers of structured population dynamics in changing environments. *Ecology Letters*, *19*(9), 1023–1031. https://doi.org/10.1111/ele.12628

Lande, R., Engen, S., & SÆther, B.-E. (2003). Demographic and environmental stochasticity. In R. Lande, S. Engen, & B.-E. Saether (Eds.), *Stochastic Population Dynamics in Ecology and Conservation* (p. 0). Oxford University Press. https://doi.org/10.1093/acprof:oso/9780198525257.003.0001

Low, M., Arlt, D., Eggers, S., & Pärt, T. (2010). Habitat-specific differences in adult survival rates and its links to parental workload and on-nest predation. *Journal of Animal Ecology*, *79*(1), 214–224. https://doi.org/10.1111/j.1365-2656.2009.01595.x

Maldonado-Chaparro, A. A., Blumstein, D. T., Armitage, K. B., & Childs, D. Z. (2018). Transient LTRE analysis reveals the demographic and trait-mediated processes that buffer population growth. *Ecology Letters*, *21*(11), 1693–1703. https://doi.org/10.1111/ele.13148

Millon, A., Lambin, X., Devillard, S., & Schaub, M. (2019). Quantifying the contribution of immigration to population dynamics: a review of methods, evidence and perspectives in birds and mammals. *Biological Reviews*, *94*(6), 2049–2067. https://doi.org/10.1111/brv.12549

Nater, C., Burgess, M., Coffey, P., Harris, B., Lander, F., Price, D., Reed, M., & Robinson, R. (2022). Spatial consistency in drivers of population dynamics of a declining migratory bird. *Journal of Animal Ecology*, *92*. https://doi.org/10.1111/1365-2656.13834

Öberg, M., Arlt, D., Pärt, T., Laugen, A. T., Eggers, S., & Low, M. (2015). Rainfall during parental care reduces reproductive and survival components of fitness in a passerine bird. *Ecology and Evolution*, *5*(2), 345–356. https://doi.org/10.1002/ece3.1345

Paquet, M., Arlt, D., Knape, J., Low, M., Forslund, P., & Pärt, T. (2019). Quantifying the links between land use and population growth rate in a declining farmland bird.

Ecology and Evolution, *9*(2), 868–879. https://doi.org/10.1002/ece3.4766

Paquet, M., Knape, J., Arlt, D., Forslund, P., Pärt, T., Flagstad, Ø., Jones, C. G., Nicoll, M. A. C., Norris, K., Pemberton, J. M., Sand, H., Svensson, L., Tatayah, V., Wabakken, P., Wikenros, C., Åkesson, M., & Low, M. (2021). Integrated population models poorly estimate the demographic contribution of immigration. *Methods in Ecology and Evolution*, *12*(10), 1899–1910. https://doi.org/10.1111/2041-210X.13667

Pärt, T. (2001). The effects of territory quality on age-dependent reproductive performance in the northern wheatear, Oenanthe oenanthe. *Animal Behaviour*, *62*(2), 379–388. https://doi.org/10.1006/anbe.2001.1754

Plard, F., Fay, R., Kéry, M., Cohas, A., & Schaub, M. (2019). Integrated population models: powerful methods to embed individual processes in population dynamics models. *Ecology*, e02715. https://doi.org/10.1002/ecy.2715

Rees, M., & Ellner, S. P. (2009). Integral projection models for populations in temporally varying environments. *Ecological Monographs*, *79*(4), 575–594. https://doi.org/10.1890/08-1474.1

Ross, B. E., & Weegman, M. D. (2022). Relative effects of sample size, detection probability, and study duration on estimation in integrated population models. *Ecological Applications*, *32*(8), e2686. https://doi.org/10.1002/eap.2686

Schaub, M., & Kéry, M. (2021). *Integrated Population Models: Theory and Ecological Applications with R and JAGS* (1st edition). Academic Press.

Simpson, D., Rue, H., Riebler, A., Martins, T. G., & Sørbye, S. H. (2017). Penalising Model Component Complexity: A Principled, Practical Approach to Constructing Priors. *Statistical Science*, *32*(1), 1–28. https://doi.org/10.1214/16-STS576

Steiner, U. K., Tuljapurkar, S., & Roach, D. A. (2021). Quantifying the effect of genetic, environmental and individual demographic stochastic variability for population dynamics in Plantago lanceolata. *Scientific Reports*, *11*(1), Article 1. https://doi.org/10.1038/s41598-021-02468-9

Valpine, P. de, Turek, D., Paciorek, C. J., Anderson-Bergman, C., Lang, D. T., & Bodik, R. (2016). Programming with models: writing statistical algorithms for general model structures with NIMBLE. *Journal of Computational and Graphical Statistics*, *0*(ja), 1–28. https://doi.org/10.1080/10618600.2016.1172487

Ver Hoef, J. M. (2012). Who Invented the Delta Method? *The American Statistician*, *66*(2), 124–127. https://doi.org/10.1080/00031305.2012.687494

Weegman, M. D., Arnold, T. W., Dawson, R. D., Winkler, D. W., & Clark, R. G. (2017). Integrated population models reveal local weather conditions are the key drivers of population dynamics in an aerial insectivore. *Oecologia*, *185*(1), 119–130. https://doi.org/10.1007/s00442-017-3890-8

Zhao, Q., Heath-Acre, K., Collins, D., Conway, W., & Weegman, M. D. (2021). Integrated population modelling reveals potential drivers of demography from partially aligned data: a case study of snowy plover declines under human stressors. *PeerJ*, *9*, e12475. https://doi.org/10.7717/peerj.12475

Appendix A - IPM details

Study system and data filtering

We used field data from a long-term population study of northern wheatears (*Oenanthe oenanthe*), a migratory Passerine bird species wintering in the Sahel region (Arlt et al., 2015; Cramp, 1988) and breeding in an agricultural landscape near Uppsala in Sweden. The study site is located south east of Uppsala, (59,500 N, 17,500 E), and covers an area of 60 km2 with 230 territory sites that have been occupied by wheatears at least once since 1993 when the yearly monitoring started. About 100–180 pairs breed annually in the study area. Demographic data of individuals used in this study, however, were collected from a smaller central part of the study area (c. 40 km2, 179 territory sites and 70-100 pairs breeding annually) to achieve more precise estimates of survival rates of individuals dispersing short distances between years. For details of the study system, see e.g. (Arlt & Pärt, 2017; Paquet et al., 2019)

Breeding data

We split breeding performance into three separate components: the probability of a nest to survive until chicks are approximately 6 days old (i.e. early nest survival; the period starts at nest initiation and includes the egg stage as well as the period where females frequently incubate small nestlings), the number of chicks in the nest at that age, and the individual survival probability of chicks from an age of 6 days to fledging (i.e. nestling survival). This was chosen to match the collection of different types of information on reproduction (Arlt et al., 2008; Pärt, 2001). If the nest was accessible, chicks were ringed and counted when they were approximately 6 days old. For the

subset of nests that could be ringed, we therefore have information about the nest still being alive when the chicks were 6 days old, and the number of chicks in the nest. At the time of fledging, defined as the time when chicks are around 15 days old, all nests were checked for signs of activity (chick seen or alarming parents) to determine fledging success. The fledging success data are therefore binary indicating whether at least one chick was still alive at the time of fledging. The breeding model was assembled from these pieces of information.

We assume that nests survive until chicks are 6 days old with probability $\nu_{a,t}$ (early nest survival, including mainly the incubation period), where survival is defined as at least one surviving chick, and a denotes whether the male of the nest is young or old. Given early nest survival until chicks are 6 days old, we assume that chicks are ringed with probability $p_{R,t}$, which are year dependent nuisance parameters, and that the number of chicks in the nest follows a Poisson distribution with a constant mean r. We also assume that the number of chicks in the nest is independent of whether or not chicks were ringed.

A chick that is 6 days old survives until fledging (15 days) with probability ψ_t (nestling survival). We assume that the survival of chicks during this period was composed of two parts, a time-varying probability of complete nest failure ψ_t (e.g. due to predation) and a constant probability ζ of individual chick death that is independent among siblings. We then model breeding success as the probability that the nest does not completely fail and at least one chick survives until 15 days after hatching, so that the probability of breeding success in a nest with m 6 day old chicks is $\psi_t(1-(1-\zeta)^m)$.

We then model the joint data, (f, m), for each nest where f is the binary fledging success and m is the number of chicks ringed in the nest (which is zero if the nest could not be accessed). For ringed nests ($m > 0$), we know that the nest survived until chicks were approximately 6 days old and therefore

$$f|m \ \sim \text{Bernoulli}(\psi_t(1-(1-\zeta)^m))$$

For unringed nests we have

$$P(f = 1|m = 0) = \frac{P(f = 1, m = 0)}{P(m = 0)}$$

The probability that a nest is not ringed $P(m = 0)$ is 1 minus the probability that it

is ringed:

$$P(m = 0) = 1 - \nu_{a,t} p_{R,t}$$

The joint probability is

$$P(f = 1, m = 0) = \nu_{a,t}(1 - p_{R,t}) \sum_{x>0} (\psi_t(1 - (1 - \zeta)^x)) \, \text{Poisson}(x; r)$$

where the sum is over the possibilities for the number of chicks in the nest, and $\text{Poisson}(x; r)$ is the Poisson probability of x chicks when the mean is r (i.e. $\text{Poisson}(x; r) = r^x \exp(-r)/x!$). By combining the above,

$$f|m = 0 \sim \text{Bernoulli}\left(\nu_{a,t} \frac{1 - p_{R,t}}{1 - \nu_{a,t} p_{R,t}} \sum_{x>0} (\psi_t(1 - (1 - \zeta)^x)) \, \text{Poisson}(x; r)\right).$$

To finalise the joint model of (f, m), we also need to determine the marginal distribution of m. For this, we have that m is larger than 0 with probability $\nu_{a,t} p_{R,t}$ as above, and given $m > 0$, $m \sim \text{Poisson}(r)$. For simplicity we did not zero truncate the Poisson distribution since the observed mean of the number of chicks ringed is large enough (5.3) that zeros are unlikely.

The assumption that temporal variation in nestling survival is driven entirely by the complete nest failure probability ψ_t is somewhat arbitrary. We therefore alternatively considered a model where the temporal variation is instead driven by the other component ζ_t and where the probability of complete nest failure is constant over time. Results from this model are presented in Appendix B.

Covariates Temporal variation in early nest survival, $\nu_{a,t}$, was modelled at the logit scale with an intercept, temperature and rainfall as covariates, and a random residual term. Daily temperature and rainfall were obtained from a weather station in Ultuna, approximately 10 kms from the study area. The covariates were computed as the daily mean of temperature between May 14 and June 14 each year, a period covering incubation for a majority of individuals. These covariates were included because poor weather conditions (low temperature and/or high precipitation) could potentially affect survival of young in the first days or the ability of parents to care for the nest (Öberg et al., 2015). All coefficients were estimated as different for the two age classes (young

and old male parent), and random effects were assumed independent between the age classes.

Temporal variation in nestling survival, ψ_t, was modelled similarly to early nest survival, but without dependence on the age of the parent, and mean daily temperature and rainfall were computed over the period from June 2 to June 24, covering the nestling survival period for a majority of individuals. The motivation for the covariates is the expectation that high temperature and low precipitation could make it easier for parents to find food for the chicks (Öberg et al., 2015).

Mark-resighting data

Birds were ringed with colour rings, either as chicks in the nest or when trapped as adults. Marked birds are then resighted and identified from the colour marks in following years (and sometimes also re-trapped). We only consider trapping and resightings of males. However, chicks marked in the nest cannot be sexed in the hand. We therefore include all chicks marked, but they will only occur as resighted in later years if they are male.

We use a CJS formulation for these data with time and age dependent survival probabilities modelled with covariates and random effects, and temporally constant but age dependent (young and old) detection probabilities.

We parametrized survival in the first year (for birds ringed in the nest) as a product of nestling survival (survival from ringing until fledging, ψ_t above) and first year survival (survival from fledging until returning and establishing a territory the next year, $\phi_{0,t}$). As we only consider resightings of males and the sex of birds is unknown in their first year, the first year survival probability, $\phi_{0,t}$, includes the probability that the bird is a male. Since we expect an even sex ratio at the time of ringing, actual apparent survival of male chicks should be close to $2\phi_{0,t}$. Annual apparent survival of young males (one year old) until establishing a territory the next year is denoted $\phi_{1,t}$ and annual apparent survival of old males (2+ years) is denoted $\phi_{2,t}$.

Covariates For first year survival, $\phi_{0,t}$, we included a rainfall index for the wintering area in Sahel, and population size (i.e. density dependence) in the study area as covariates. The rainfall index was computed as the mean of a monthly index from June

through October (JISAO, 2018) in the same year as the birds arrive in the wintering area. This coincides with the rainy season in Sahel which affects how dry the winter months will be, and thereby vegetation development and potentially foraging conditions. Northern wheatears are known to winter in the Sahel (Cramp, 1988), and birds from our study population winter in a relatively large part of the Western African Sahel (Arlt et al., 2015). Rain conditions are fairly homogeneous across large parts of the Western and Eastern Sahel regions, and we therefore expect the Sahel rainfall index to be associated with the wintering conditions at a regional scale for birds from the study population.

Density dependence was included under the hypothesis that chicks born in a year with a large breeding population may be less able to return to the study area to establish their own nest in the following year. Population density was included as the total abundance ($n_{1,t} + n_{2,t}$), and was transformed by removing 90 and dividing the result by 10 to roughly center and scale the covariate.

For survival of young and old males we included temperature and rainfall during the nestling period (June 8 to June 24 as defined above) as well as the Sahel rainfall index. The rationale behind the covariates for the nestling period was that they may affect the amount of effort required by parents to raise young, which may in turn affect survival (Low et al., 2010).

All above survival probabilities were modelled at the logit scale and also included intercepts and residual random effects, and all with different parameters for each age. Random effects were also assumed independent across the different ages.

Census data

Census data on the number of occupied breeding territories were collected by continuously monitoring potential territory and nest sites during the breeding season. For almost all breeding pairs we also know the age of the male. We therefore use the number of territories occupied by young and old males as census data, which provide direct information about annual population growth. We assume that counts follow a Poisson distribution:

$$n_{a,t}^{\text{obs}} \sim \text{Poisson}(n_{a,t})$$

for both young ($a = 1$) and old ($a = 2$) males. The $n_{a,t}$ are assumed to follow the population process governed by the vital rates in Table 1, and with demographic stochasticity incorporated by drawing the number of surviving nests, juveniles, and young and old males using binomial distributions, and the number of young in nests and immigrants using Poisson distributions (see model code in Supplement 1).

Due to the large number of visits to the study area each season, we believe census errors to be small and a Poisson distribution should have enough variance to capture census errors.

Appendix B - Goodness of fit and an alternative model

Alternative model specification

As mentioned in the main text, we tested a different specification of the model for breeding success (Appendix A) where the probability of breeding success (at 15 days after hatching) from the time of ringing was $\psi(1-(1-\zeta_t)^m)$. This model has temporal variation (covariates and random effects) in the probability of individual chick death (ζ_t) instead of in the probability of complete nest failure (ψ). All other aspects of the alternative model were identical to those of the model in the main text.

Results from this model differ from those in the main text in that there is a large contribution from nestling survival to variation in growth, and the contribution from first year survival is reduced (Fig. 6). The reason for this seems to be that a higher temporal variation in ζ_t is required to capture temporal variation in breeding success than in the model with variation in ψ. This is because $1-(1-\zeta_t)^m$ is closer to 1 than ζ_t and therefore the variation in $1-(1-\zeta_t)^m$ is restricted, which needs to be countered by a higher variance in ζ_t.

The goodness of fit checks in the next subsection did not show a clear preference for either of the two model formulations over the other.

Goodness of fit

We assessed goodness of fit using posterior predictive p-values with Freeman-Tukey goodness of fit statistics for breeding success and mark recapture data. We simulated the replicate data for each MCMC iteration starting from the random effects values,

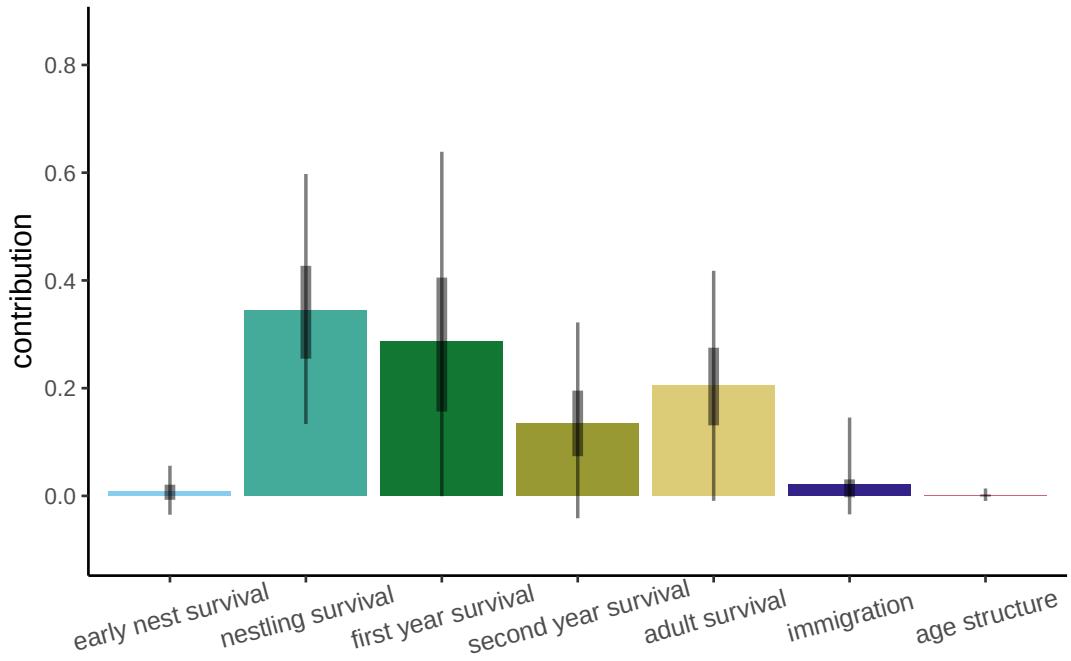

Figure 6: Total relative contributions to environmental variance in the realized growth rate for each vital rate (summed across all linear predictor components of the vital rates) for the alternative model specification. Error bars show 50% (thick) and 95% (thin) credible intervals.

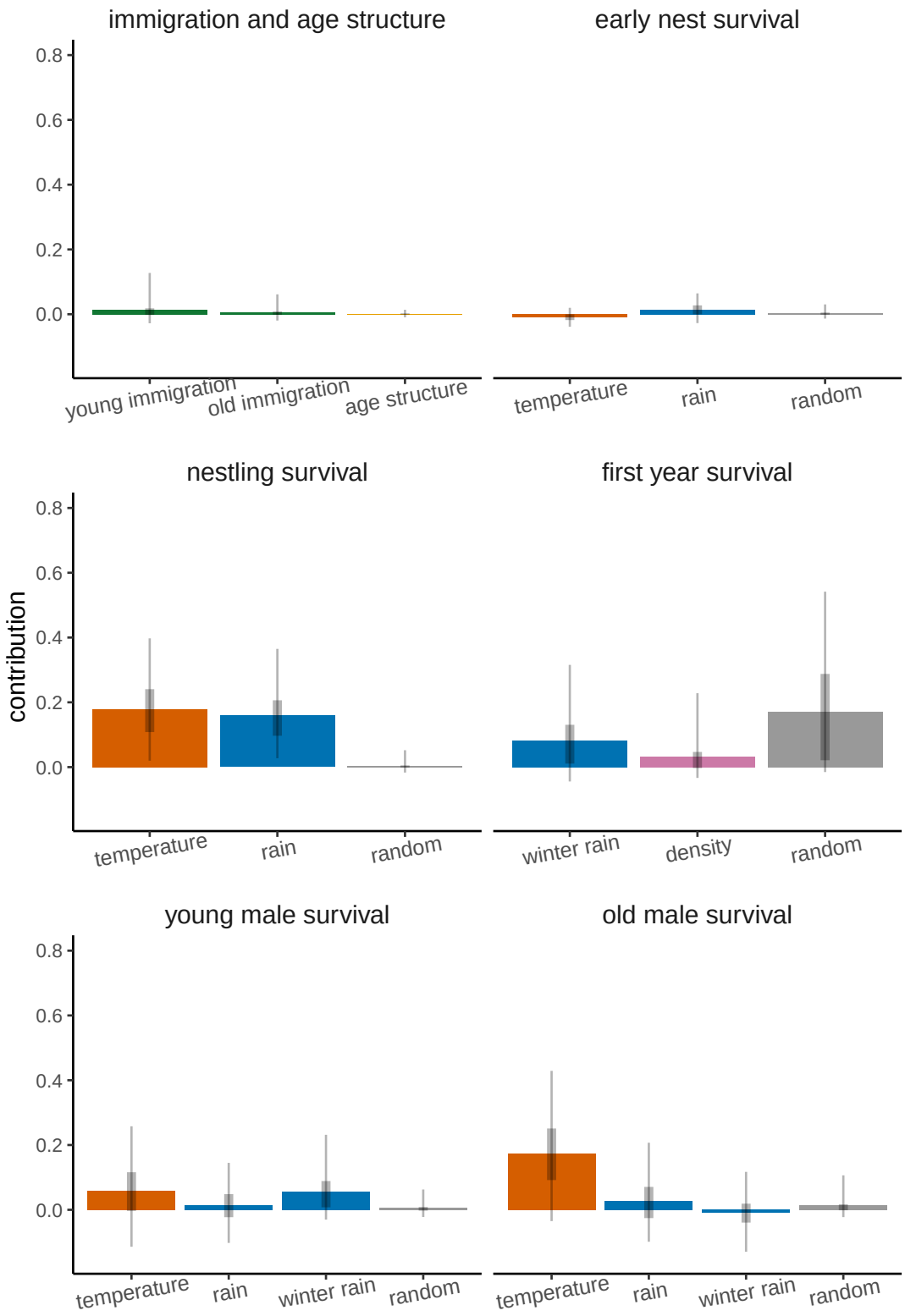

Figure 7: Relative contributions to environmental variation in the realized growth rate from all linear predictor components and vital rates in the alternative model. Error bars show 50% (thick) and 95% (thin) credible intervals.

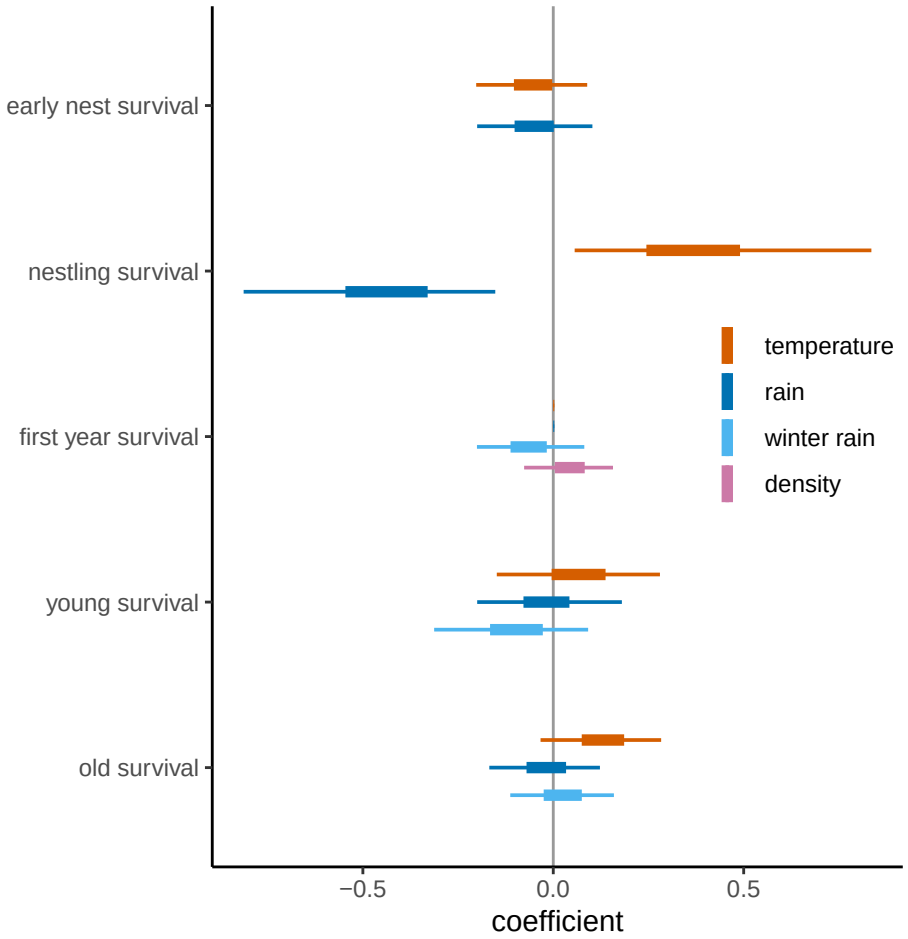

Figure 8: Estimated slopes for all environmental covariates on vital rates in the alternative model. Error bars show 50% (thick line) and 95% (thin line) credible intervals.

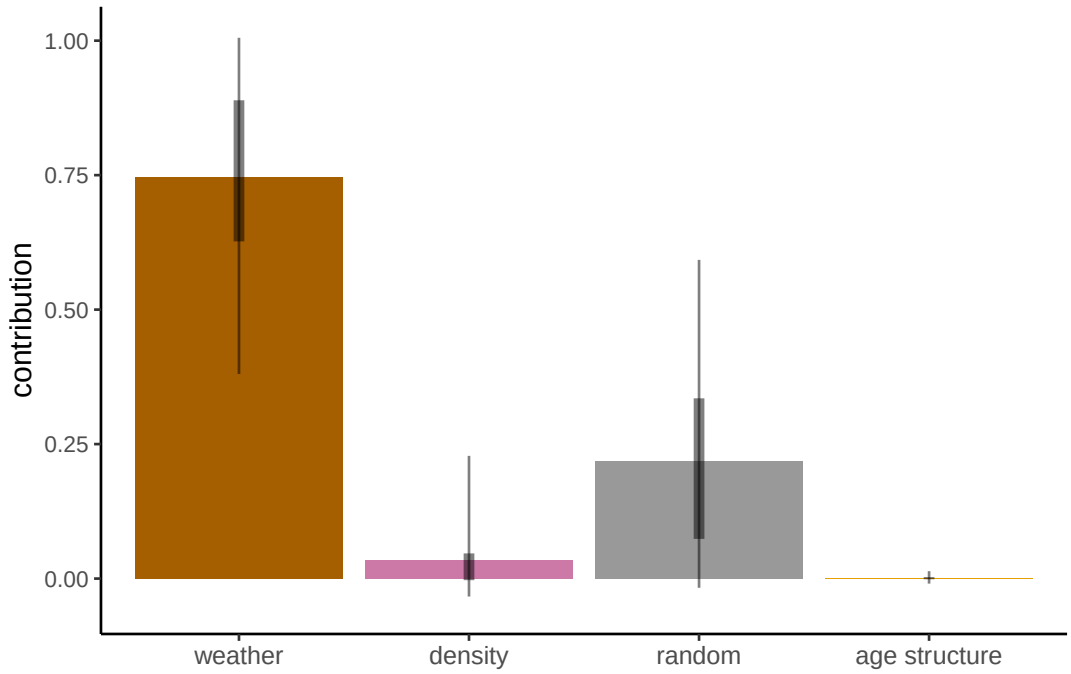

Figure 9: Relative contributions from weather (rainfall and temperature), population density, random effects (including for immigration), and age structure to environmental variance in realized growth in the alternative model. Error bars show 50% (thick) and 95% (thin) credible intervals.

i.e. we conditioned on the random effects rather than drawing new values for the temporal variation.

The Freeman-Tukey statistic is

$$\sum_i (\sqrt{z_i} - \sqrt{E(z_i)})^2$$

where z_i is an aggregation of binomial variables over a group i and $E(z_i)$ is the expected value of z_i.

For breeding success, we used the Freeman-Tukey statistic for both ringed and unringed nests. For ringed nests, we aggregated the number of successes by both year and the number of ringed chicks, giving two discrepancy metrics. For unringed nests (where the number of chicks is not known) we aggregated only by year.

For the mark recapture data we computed Freeman Tukey statistics for the number of recaptured young and old males respectively, both aggregated by year.

The above statistics are shown in Fig. 10 for the model in the main text and for the alternative model in Fig. 11. As the p-values are very similar between the two models, it appears difficult to distinguish between them.

The fit of the Poisson model of the number of chicks in the nest at time of ringing was done separately by visually comparing the empirical distribution of the number of chicks ringed per nest to the fitted Poisson model, which has a mean of 5.3. The distribution of the number of chicks is underdispersed relative to the Poisson, as the maximum number of observed chicks was 8. As mentioned in the main text, we were not successful with attempts at using a multinomial distribution for the number of chicks and stayed with the Poisson despite the underdisperion. This may lead to somewhat higher estimation uncertainty, and could inflate the contribution of demographic stochasticity to some extent.

The fit of the count model was checked visually by comparing the estimated population trajectory to observed population totals (Fig 1).

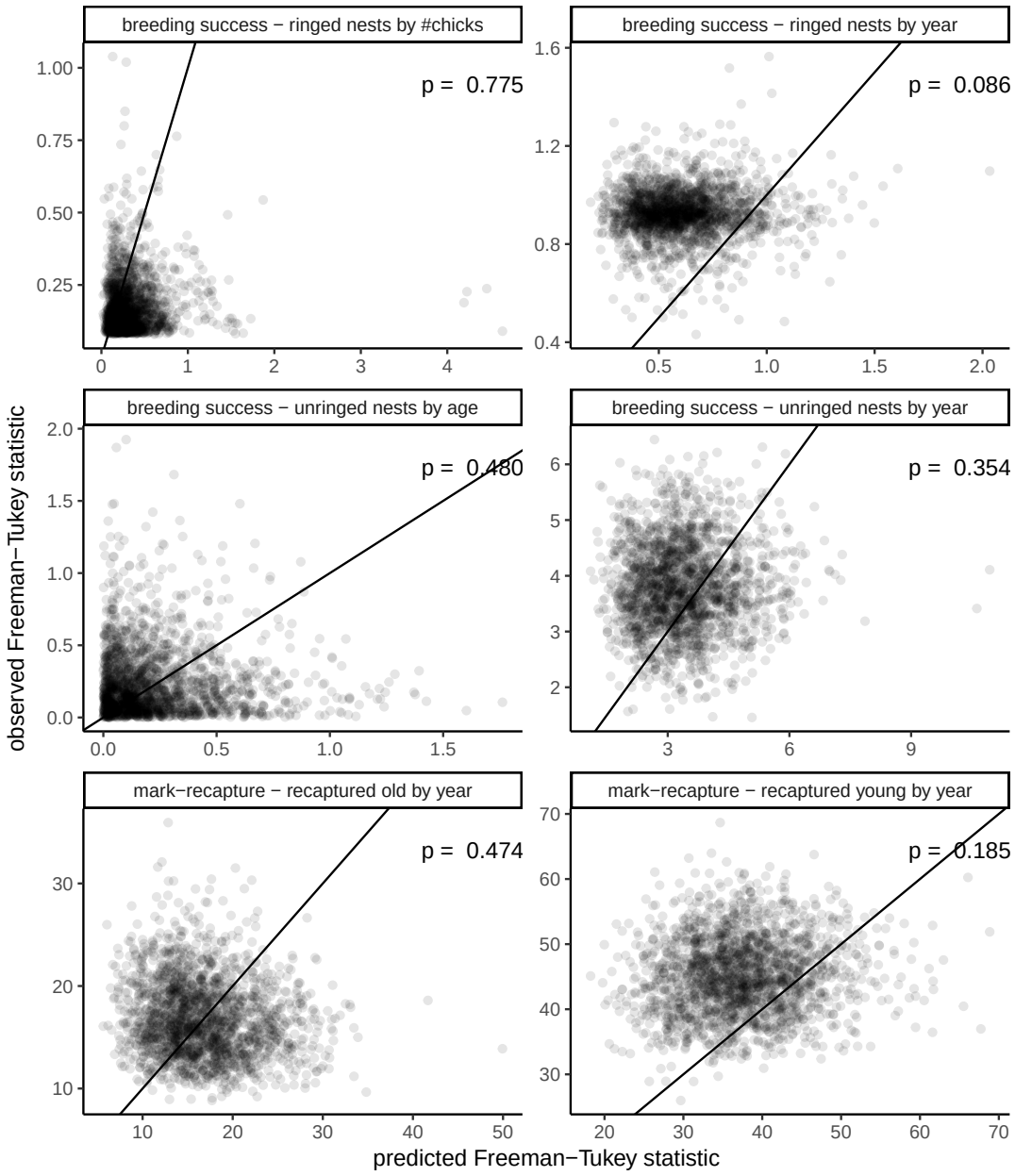

Figure 10: Observed versus predicted (via posterior simulation) values of the Freeman-Tukey goodness of fit statistics across the posterior distribution for the model in the main text. The resulting Bayesian p-values are also shown.

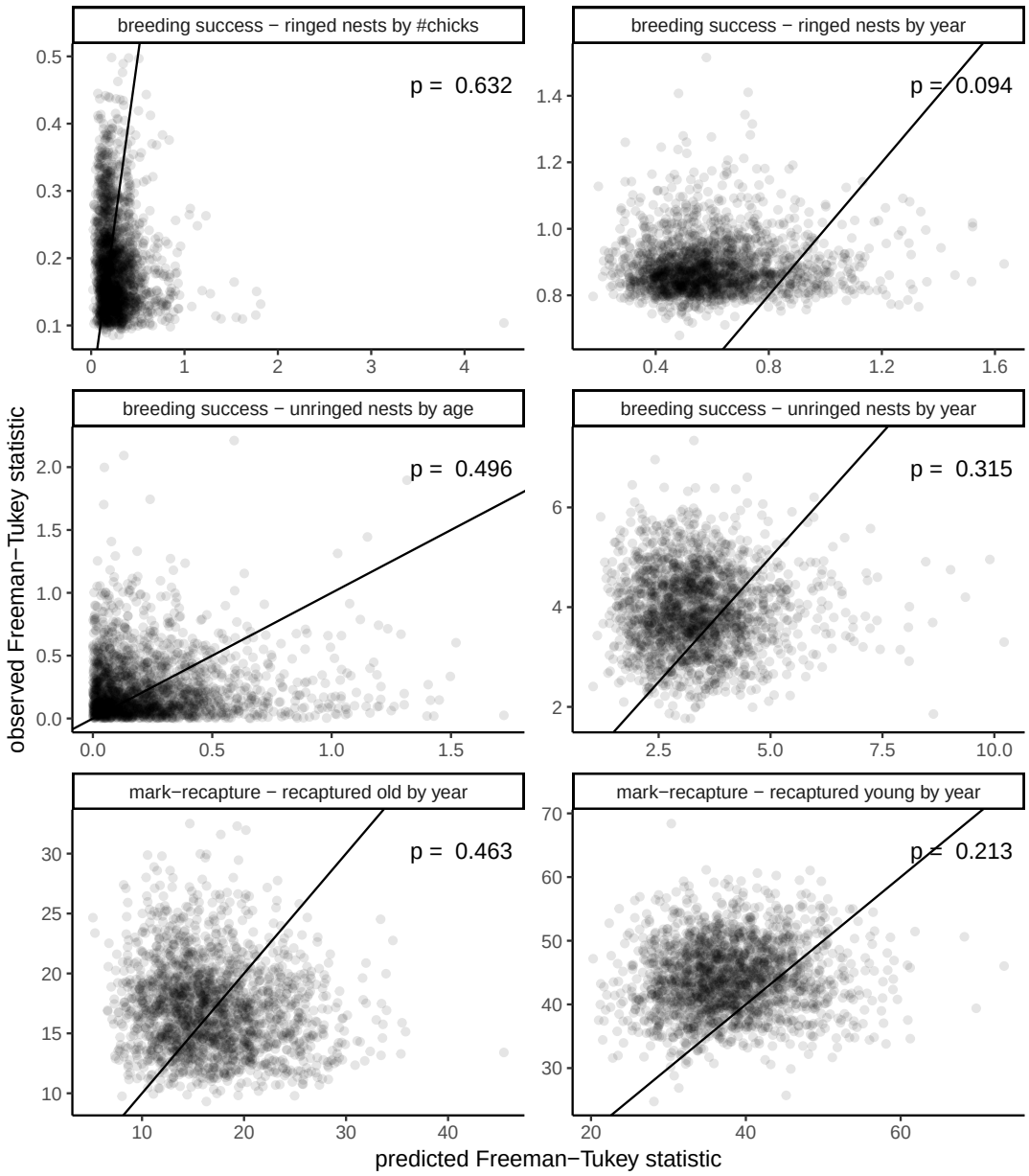

Figure 11: Observed versus predicted (via posterior simulation) values of the Freeman-Tukey goodness of fit statistics across the posterior distribution for the alternative model. The resulting Bayesian p-values are also shown.